Mutual Sensitization of the Oxidation of Nitric Oxide and a Natural Gas Blend in a JSR at Elevated Pressure: Experimental and Detailed Kinetic Modeling Study†

Philippe Dagaut* and Guillaume Dayma

CNRS, Laboratoire de Combustion et Systèmes Réactifs, 1C, Avenue de la Recherche Scientifique, 45071 Orléans Cedex 2, France

Received: August 12, 2005; In Final Form: November 7, 2005

The mutual sensitization of the oxidation of NO and a natural gas blend (methane−ethane 10:1) was studied experimentally in a fused silica jet-stirred reactor operating at 10 atm, over the temperature range 800−1160 K, from fuel-lean to fuel-rich conditions. Sonic quartz probe sampling followed by on-line FTIR analyses and off-line GC-TCD/FID analyses were used to measure the concentration profiles of the reactants, the stable intermediates, and the final products. A detailed chemical kinetic modeling of the present experiments was performed yielding an overall good agreement between the present data and this modeling. According to the proposed kinetic scheme, the mutual sensitization of the oxidation of this natural gas blend and NO proceeds through the NO to NO_2 conversion by HO_2, CH_3O_2, and $C_2H_5O_2$. The detailed kinetic modeling showed that the conversion of NO to NO_2 by CH_3O_2 and $C_2H_5O_2$ is more important at low temperatures (ca. 820 K) than at higher temperatures where the reaction of NO with HO_2 controls the NO to NO_2 conversion. The production of OH resulting from the oxidation of NO by HO_2, and the production of alkoxy radicals via $RO_2 + NO$ reactions promotes the oxidation of the fuel. A simplified reaction scheme was delineated: $NO + HO_2 \rightarrow NO_2 + OH$ followed by $OH + CH_4 \rightarrow CH_3 + H_2O$ and $OH + C_2H_6 \rightarrow C_2H_5 + H_2O$. At low-temperature, the reaction also proceeds via $CH_3 + O_2 (+ M) \rightarrow CH_3O_2 (+ M)$; $CH_3O_2 + NO \rightarrow CH_3O + NO_2$ and $C_2H_5 + O_2 \rightarrow C_2H_5O_2$; $C_2H_5O_2 + NO \rightarrow C_2H_5O + NO_2$. At higher temperature, methoxy radicals are produced via the following mechanism: $CH_3 + NO_2 \rightarrow CH_3O + NO$. The further reactions $CH_3O \rightarrow CH_2O + H$; $CH_2O + OH \rightarrow HCO + H_2O$; $HCO + O_2 \rightarrow HO_2 + CO$; and $H + O_2 + M \rightarrow HO_2 + M$ complete the sequence. The proposed model indicates that the well-recognized difference of reactivity between methane and a natural gas blend is significantly reduced by addition of NO. The kinetic analyses indicate that in the NO-seeded conditions, the main production of OH proceeds via the same route, $NO + HO_2 \rightarrow NO_2 + OH$. Therefore, a significant reduction of the impact of the fuel composition on the kinetics of oxidation occurs.

1. Introduction

Previous studies on the kinetics of the interactions between nitric oxide (NO) and a variety of fuels have demonstrated that the ignition of simple fuels is promoted by traces of nitric oxide[1,2] whereas the NO to NO_2 conversion is favored. This phenomenon was interpreted in terms of a mutual sensitization of the oxidation of the fuel and of nitric oxide. NO promotes the oxidation of the fuel and the oxidation of NO into NO_2 is promoted through the radical pool generated from hydrocarbon's oxidation. Previous kinetic studies have mainly been performed using plug-flow reactors (PFR). They investigated the promoting effect of NO on the oxidation of hydrogen,[3] and hydrocarbons ranging from methane to *n*-pentane,[4−13] whereas several other studies concentrated on the promotion of the oxidation of NO to NO_2 by hydrocarbons.[11,14−16] The kinetics of such systems were previously presented.[4,5,11,13,17,18] Actually, taking into account this chemistry is important in several practical environment among which one should cite the following: (i) the NO−NO_2 conversion by hydrocarbons in recent NO_x-reduction strategies, (ii) the modeling of combustion in flameless burners,[19] and (iii) the modeling of combustion in engines involving exhaust-gas recirculation (EGR),[20] such as modern Diesel engines, and more importantly, HCCI engines. In such engines, a variable fraction of the exhaust gas is readmitted into the engine, reducing the temperature in the combustion chamber, and in turn the formation of thermal-NO. The other effect of EGR is the reduction of ignition delays in the engine by a NO_x-promoted oxidation of the fuel.[21] It is recognized that the firing of HCCI engines is critically controlled by the kinetics of the ignition of the fuel. It is thus of major importance to take into account the promoting effect of NO_x on this process to better control the ignition in such engines. However, until recently, no data were available for such reactions under high-pressure conditions[18,21] and most of the data were obtained in PFR, where back-mixing is minimal whereas it is important in practical systems. Furthermore, all the previous studies concerned the oxidation of pure fuels, not mixtures of hydrocarbons, whereas it is well-known[22,23] that the presence of higher hydrocarbons in natural gas is responsible for its higher reactivity[22,23] relative to that of methane (see Figure 1).

Therefore, a series of experiments was performed at 1 to 10 atm to evaluate the kinetics of the NO-sensitized oxidation of methane[18] and higher hydrocarbons[21,25] using a JSR. The present data, involving a methane−ethane mixture (a natural gas blend, NGB), were used to further validate a detailed chemical kinetic

† Part of the special issue "David M. Golden Festschrift".

* Author for correspondence. E-mail: dagaut@cnrs-orleans.fr. Telephone: (33) 238 25 54 66. Fax: (33) 238 69 60 04.

10.1021/jp054535w CCC: $33.50
Published on Web 12/09/2005

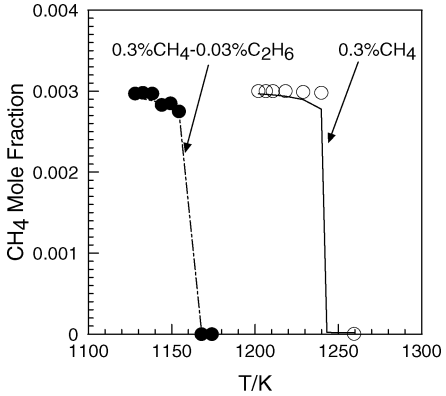

Figure 1. Comparison of the reactivity of methane and a methane−ethane natural gas blend mixture in a JSR at 1 atm, $\varphi = 0.5$, $t = 140$ ms.[22] The symbols and the continuous lines refer respectively to the data and the simulations.

reaction mechanism proposed earlier for the interaction between NO and pure hydrocarbons,[18,21,25] and clarify the relative importance of the reactions of NO with HO_2 and RO_2 (methylperoxy and ethylperoxy in the present case) in the NO-sensitized oxidation of natural gas under high pressure. The sensitivity of the rate of oxidation to the composition of natural gas in the presence of NO had still to be clarified; this is also theoretically investigated here via a detailed kinetic modeling.

2. Experimental Section

The experimental setup consisted of a spherical fused silica jet-stirred reactor (JSR)[26] located inside a regulated electrical resistance system of ≈1.5 kW, surrounded by insulating material and fitted into a stainless steel pressure-resistant jacket. It can operate at pressures up to 10 atm. High purity reactants were used: methane (99.9995% pure), ethane (99.9995% pure), NO (>99.995% pure), and oxygen (99.995% pure). A NGB mixture of 10% in nitrogen (99.9995% pure) and a mixture of 10% NO in nitrogen (99.995% pure) were used. They flowed separately through a two-hole alumina capillary (1 mm i.d.) until the mixing point located just before the entrance of the injectors. The flow rates were measured and regulated by thermal mass-flow controllers. The reactants were diluted by a flow of nitrogen (<50 ppm of O_2; <1000 ppm of Ar; <5 ppm of H_2) and mixed at the entrance of the injectors after preheating. Residence time distribution indicated that the reactor is operating under macromixing conditions. Therefore, we assumed a perfectly stirred-reactor model could be used. As in previous work,[7,9,18,25] a good thermal homogeneity was measured along the entire vertical axis of the reactor using a thermocouple. We used a Pt/Pt−Rh 10%, 0.1 mm diameter located inside a thin-wall fused-silica tube, <0.5 mm, to prevent catalytic reactions on the metallic wires. Temperature gradients of <8 K were typically measured. Because of the high degree of dilution under which we operated, the temperature rise due to the reaction was generally <30 K. As in refs 7, 9, 18, and 25, a sonic quartz probe was used for sampling and collecting low-pressure samples of the reacting mixtures in 1 L Pyrex bulbs at ca. 40 mbar for immediate gas chromatography (GC) analyses. To improve the GC detection, the samples were pressurized at 0.8 bar before injection into the GC column, using a glass homemade piston. Capillary columns of 0.53 mm i.d. (Poraplot U and Molecular sieve 5A, carrier gas helium) were used with a thermal conductivity detector (TCD) and a flame ionization detector (FID) for the measurements of gases, but hydrogen was measured by TCD on a separate system (Carboplot P7, carrier gas nitrogen). On-line Fourier transform infrared (FTIR) analyses of the reacting gases were also performed by connecting the sampling probe to a temperature controlled (140 °C) gas cell (10 m path length) via a Teflon heated line (130 °C). The sample pressure in the cell was 0.2 bar. This analytical equipment allowed the measurements of methane, ethane, ethene, acetylene, O_2, H_2O, NO, NO_2, N_2O, CO, CH_2O, CH_3OH, and CO_2. As previously,[7,9,18,25] very good agreement between the GC and FTIR analyses was found for the compounds measured by both techniques (methane, CO, CO_2). Carbon balance was checked for every sample and found to be good within < 5%. The mole fractions of NO and NO_2 were determined to within ±5−15 ppm.

3. Chemical Kinetic Modeling

The kinetic modeling was performed using the PSR computer code.[27] The proposed reaction mechanism is the kinetic scheme developed for the mutual oxidation of NO−methane,[18] NO−ethane, and NO−ethene,[25] deriving from previous modeling (NO−ethane,[7] DME−NO,[9] and NO-reburning by C_1 to C_4 hydrocarbons and syngas[28]). A low-temperature kinetic reaction sub-mechanism including the interactions of NO and NO_2 with hydrocarbons is included. A subset of the kinetic scheme is presented in Table 1. The full kinetic reaction mechanism, including thermochemical data, is available from the corresponding author. The pressure dependencies of unimolecular reactions and of some pressure-dependent bimolecular reactions were taken into account (i.e., $k(P, T)$). The rate constants for the reverse reactions were computed from the forward rate constants and the appropriate equilibrium constants calculated using thermochemical data.[7,9,28] In the literature, the heat of formation $\Delta H°_{298}$ (CH_3O_2) ranges from 10.46 to 47.28 kJ/mol. Tests were performed of the influence of the heat of formation of CH_3O_2 on the predicted mole fractions by varying the heat of formation from 10.46 to 25.52 kJ/mol. They showed that increasing $\Delta H°_{298}$ (CH_3O_2) resulted in a minor reduction of the reactivity accompanied by a lower NO−NO_2 conversion, in agreement with,[5,18] and increased computed methylperoxy mole fractions. The value of 17.99 kJ/mol[17,28] was used for $\Delta H°_{298}$ (CH_3O_2) whereas for CH_3NO_2 the heat of formation was taken to be −74.68 kJ/mol as in ref 13. As reported previously,[18] the computations were significantly sensitive to this parameter. The use of the value of −70.46 kJ/mol[11] would result in a poor prediction of the NO−NO_2 conversion at low temperature.

4. Results and Discussion

A new set of experimental results, complementary to those obtained previously[18,25] for pure hydrocarbons, was obtained for the oxidation of a NGB and NGB−NO mixtures, over the temperature range 800−1160 K, for equivalence ratios ranging from $\varphi = 0.3$ to $\varphi = 1.5$ at 10 atm (Table 2). In these experiments, the residence time was set to either 250 or 800 ms. The initial concentration of methane was 2283 ppm, that of ethane was 217 ppm, and that of NO was set at either 0 or 200 ppm. Concentration profiles for the reactants (methane, ethane, NO and oxygen), stable intermediates and final products (H_2O, CO, CO_2, CH_2O, CH_3OH, NO, NO_2, C_2H_4, and C_2H_2) were measured by FTIR and GC-TCD-FID analyses. These experiments were simulated using the proposed kinetic reaction mechanism.

4.1. The Mutually Sensitized Oxidation of NO and a NGB at 10 atm. The present experiments were designed to verify the NO enhancement of the oxidation of a NGB. As depicted in Figures 2 and 3, in the presence of 200 ppm of NO, the fuel

TABLE 1: Selected Reactions from the Proposed Kinetic Reaction Mechanism[o]

reactions	*A*	*b*	*E*
$NO + HO_2 \rightleftarrows NO_2 + OH$ (144)	2.10E+12	0.0	−2008[a]
$NO_2 + H \rightleftarrows NO + OH$ (149)	1.00E+14	0.0	1515[b]
$CH_2O + NO_2 \rightleftarrows HCO + HONO$ (277)	8.00E+02	2.8	57446[c]
$H + O_2 \rightleftarrows OH + O$ (289)	1.90E+14	0.0	70341[d]
$H + O_2 + M \rightleftarrows HO_2 + M$ (290)	8.00E+17	-0.8	0[e]
$HCO + O_2 \rightleftarrows CO + HO_2$ (314)	4.72E+12	0.0	1046[f]
$CH_4 + OH \rightleftarrows CH_3 + H_2O$ (322)	1.60E+06	2.1	10301[g]
$CH_3O + M \rightleftarrows CH_2O + H + M$ (390)	4.88E+15	0.0	95282[h]
$CH_3O + O_2 \rightleftarrows CH_2O + HO_2$ (395)	2.35E+10	0.0	7481[d]
$CH_2O + OH \rightleftarrows HCO + H_2O$ (404)	1.72E+09	1.2	−1870[i]
$C_2H_6 + OH \rightleftarrows C_2H_5 + H_2O$ (411)	5.11E+06	2.1	3573[j]
$CH_3 + O_2 (+M) \rightleftarrows CH_3O_2 (+M)$ (988)	7.83E+08	1.2	0[d]
low-pressure limit	0.58E+26	-3.3	0[d]
Troe centering: 0.664, 0.1E+06, 0.10E+02			
$CH_3NO_2 (+ M) \rightleftarrows CH_3 + NO_2 (+ M)$ (1024)	1.80E+16	0.0	244764[5]
low-pressure limit	0.13E+18	0.0	175728[5]
Troe centering: 0.183, 0.1E−29, 0.10E+31			
$CH_3 + NO_2 \rightleftarrows CH_3O + NO$ (1025)	1.51E+13	0.0	0[k]
$CH_3O + NO_2 \rightleftarrows CH_2O + HONO$ (1026)	6.02E+12	0.0	9560[l]
$CH_3O + NO_2 (+ M) \rightleftarrows CH_3ONO_2 (+ M)$ (1027)	1.20E+13	0.0	0[4]
low-pressure limit	0.14E+31	-4.5	0[4]
$CH_3O + NO \rightleftarrows CH_2O + HNO$ (1028)	1.30E+14	-0.7	0[m]
$CH_3O_2 + NO \rightleftarrows CH_3O + NO_2$ (1029)	5.50E+11	0.0	−4987[n]
$C_2H_5O_2 + NO \rightleftarrows C_2H_5O + NO_2$ (1054)	3.00E+12	0.0	−1498[m]
Enhanced Collision Efficiencies[g]			
H_2O, 16.25; CO, 18.75; CO_2, 3.75; CH_4, 16.25; C_2H_6, 16.25			

[a] Howard, C. J. *J. Am. Chem. Soc.* **1980**, *102*, 6937. [b] Ko, T.; Fontijn, A. *Phys. Chem.* **1991**, *95*, 3984−3987. [c] Tsang, W.; Herron, J. T. *J. Phys. Chem. Ref. Data* **1991**, *20*, 609−663. [d] Baulch, D. L.; Cobos, C. J.; Cox, R. A.; Esser, C.; Frank, P.; Just, Th.; Kerr, J. A.; Pilling, M. J.; Troe, J.; Walker, R. W.; Warnatz, J. *J. Phys. Chem. Ref. Data* **1992**, *21*, 411−429. [e] Davidson, D. F.; Petersen, E. L.; Rohrig, M.; Hanson, R. K.; Bowman, C. T. *Proc. Combust. Inst.* **1996**, *26*, 481−488. [f] Fit to the literature data in the NIST database, 1993. [g] Warnatz, J. Rate coefficients in the C/H/O system. In *Combustion Chemistry*; Gardiner, W. C., Jr., Ed.; Springer-Verlag: New York, 1984. [h] Wantuck, P. J.; Oldenborg, R. C.; Baughcum, S. L.; Winn, K. R. *Proc. Combust. Inst.* **1989**, *22*, 973. [i] Tsang, W.; Hampson, R. F. *J. Phys. Chem. Ref. Data* **1986**, *15*, 1087. [j] Tully, F. P.; Droege, A. T.; Koszykowski, M. L.; Melius, C. F. *J. Phys. Chem.* **1986**, *90*, 691. [k] Yamada, F.; Slagle, I. R.; Gutman, D. *Chem. Phys. Lett.* **1981**, *83*, 409. [l] DeMore, W. B.; Sander, S. P.; Golden, D. M.; Hampson, R. F.; Kurylo, M. J.; Howard, C. J.; Ravishankara, A. R.; Kolb, C. E.; Molina, M. J. *JPL Publ.* **1997**, *97*−*4*. [m] Atkinson, R.; Baulch, D. L.; Cox, R. A.; Hampson, R. F., Jr.; Kerr, J. A.; Rossi, M. J.; Troe, J. *J. Phys. Chem. Ref. Data* **1997**, *26*, 521−1011. [n] Scholtens, K. W.; Messer, B. M.; Cappa, C. D.; Elrod, M. J. *J. Phys. Chem. A* **1999**, *103*, 4378 [o] $k = AT^b \exp(-E/RT)$; *A* units: mol cm s, K. *E* units: J/mol.

TABLE 2: Experimental Conditions of the Present JSR Study at 10 atm

	initial mole fractions in ppm					
φ	CH_4	C_2H_6	O_2	NO	*t*/s	*T*/K
0.5	2283	217	10700	0	0.8	950−1150
0.5	2283	217	10700	200	0.8	800−1160
1.0	2283	217	5325	200	0.8	800−1160
1.5	2283	217	3550	200	0.8	800−1160
0.3	2283	217	17750	200	0.25	800−1160
0.5	2283	217	10700	200	0.25	800−1150

starts to react at a temperature ca. 200 K lower than without NO. Almost 50% of NO is converted into NO_2 under fuel-lean conditions (Figure 3) whereas a more limited conversion was measured and predicted in stoichiometric and even more under fuel-rich conditions (Figures 4 and 5). At shorter residence time, the conversion of NO is more limited as can be seen by comparing Figures 6 and 7. The model gives very good predictions of the experimental results, as depicted in Figures 2−7. These trends are in line with the observations made in previous studies of the NO−hydrocarbons mutually sensitized oxidation.[18,25,30]

4.2. Kinetic Modeling. The kinetic reaction mechanism (147 species, 1086 reversible reactions) proposed before[18,25] was used to simulate the present experiments. As can be seen from Figures 2−7, the proposed kinetic model is in fairly good agreement with the present data, whether NO is present in the reacting mixtures or not. The proposed scheme was also successfully tested[18,25] against literature data obtained for the mutual sensitization of the oxidation of NO and methane, ethane, and ethene in PFRs.[4,11] As we were confident in the kinetic scheme used here, it served to rationalize the present results through reaction path analyses based on reaction rates of formation and consumption obtained with PSR: Computed normalized reaction rate of production (*R* with a positive sign) and reaction rate of consumption (*R* with a negative sign) were used to interpret the results (Figure 8).

In fuel-lean conditions (Figure 6 with 200 ppm of NO) and 820 K, the temperature at which the reaction starts, the three major reactions consuming NO are

$$NO + HO_2 \rightleftarrows NO_2 + OH; \quad R(NO) = -0.386 \quad (144)$$

$$CH_3O_2 + NO \rightleftarrows CH_3O + NO_2; \quad R(NO) = -0.304 \quad (1029)$$

$$C_2H_5O_2 + NO \rightleftarrows C_2H_5O + NO_2; \quad R(NO) = -0.126 \quad (1054)$$

Therefore, although reaction 144 is the major reaction consuming NO at 820 K, the combined effect of the alkylperoxy radicals through reactions 1029 and 1054 is greater. The ethylperoxy radical, produced via the oxidation of ethane, significantly participates to the oxidation of NO. Methane mostly reacts (97%) by metathesis with OH (reaction 322). Methyl radicals react predominantly with molecular oxygen yielding methylperoxy radicals.

$$CH_3 + O_2 (+ M) \rightleftarrows CH_3O_2 (+ M); \quad R(CH_3) = -0.996 \quad (988)$$

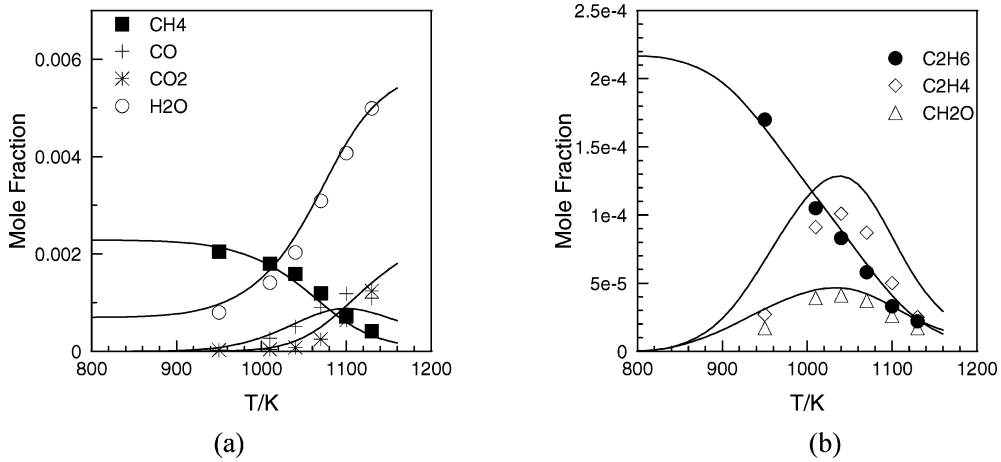

Figure 2. Oxidation of a NGB (methane−ethane 10:1) in a JSR at 10 atm under fuel-lean conditions ($\varphi = 0.5$, 2283 ppm of CH_4, 217 ppm of C_2H_6, 10700 ppm of O_2, $t = 800$ ms. The symbols and the continuous lines refer respectively to the data and the simulations (proposed scheme).

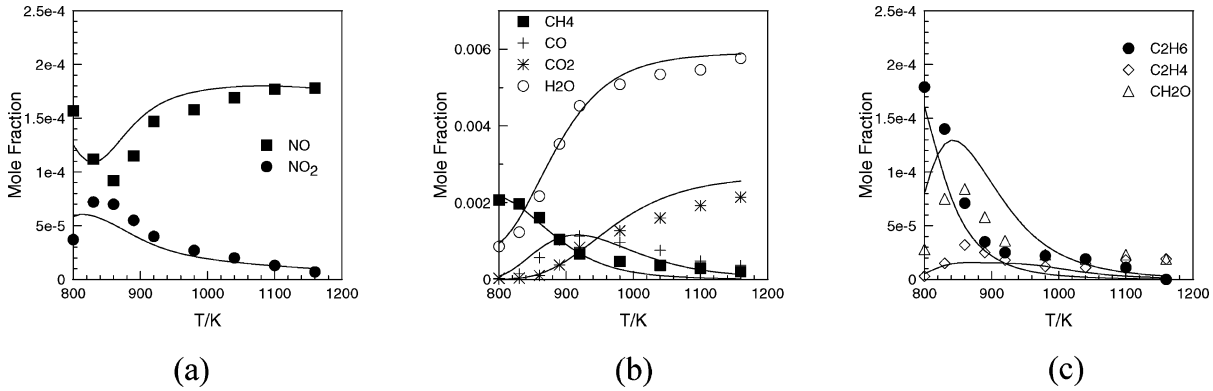

Figure 3. Mutual sensitization of the oxidation of a NGB (methane−ethane 10:1) and NO in a JSR at 10 atm: Effect of the introduction of 200 ppm of NO on the oxidation of methane under fuel-lean conditions ($\varphi = 0.5$, 2283 ppm of CH_4, 217 ppm of C_2H_6, 10700 ppm of O_2, $t = 800$ ms. The symbols and the continuous lines refer respectively to the data and the simulations (proposed scheme).

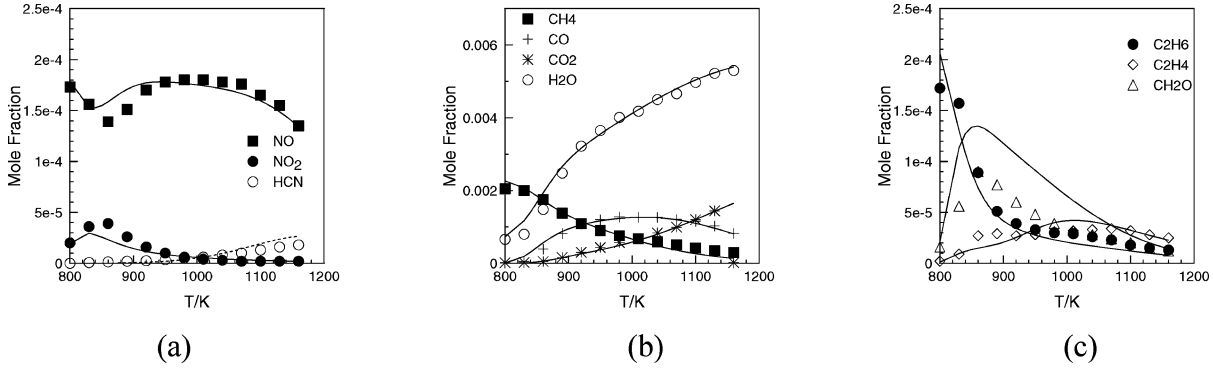

Figure 4. Mutual sensitization of the oxidation of a NGB (methane−ethane 10:1) and NO in a JSR at 10 atm: Effect of the introduction of 200 ppm of NO on the oxidation of methane in stoichiometric conditions ($\varphi = 1$, 2283 ppm of CH_4, 217 ppm of C_2H_6, 5325 ppm of O_2, $t = 800$ ms. The symbols and the continuous lines refer respectively to the data and the simulations (proposed scheme).

Methylperoxy radicals react exclusively with NO, yielding methoxy radicals.

$$CH_3O_2 + NO \rightleftarrows CH_3O + NO_2; \quad R(CH_3O_2) = -1 \tag{1029}$$

This is the main route to methoxy radicals. In these conditions, 89% of hydroperoxy radicals are produced by recombination of H and O_2 (reaction 290); a much smaller fraction is produced in

$$CH_3O + O_2 \rightleftarrows CH_2O + HO_2; \quad R(HO_2) = 0.023 \tag{395}$$

H atoms are mainly (77.7%) produced by thermal decomposition of methoxy radicals (reaction 390) whereas hydroxyl radicals, responsible for most of the methane depletion, are almost entirely produced (96%) by reaction 144. Ethane mostly reacts by metathesis with OH via reaction 411.

$$C_2H_6 + OH \rightleftarrows C_2H_5 + H_2O; \quad R(C_2H_6) = -0.97 \tag{411}$$

Ethyl radicals mostly react with molecular oxygen producing $C_2H_5O_2$ via reaction 1007.

$$C_2H_5 + O_2 \rightleftarrows C_2H_5O_2; \quad R(C_2H_5O_2) = -0.79 \tag{1007}$$

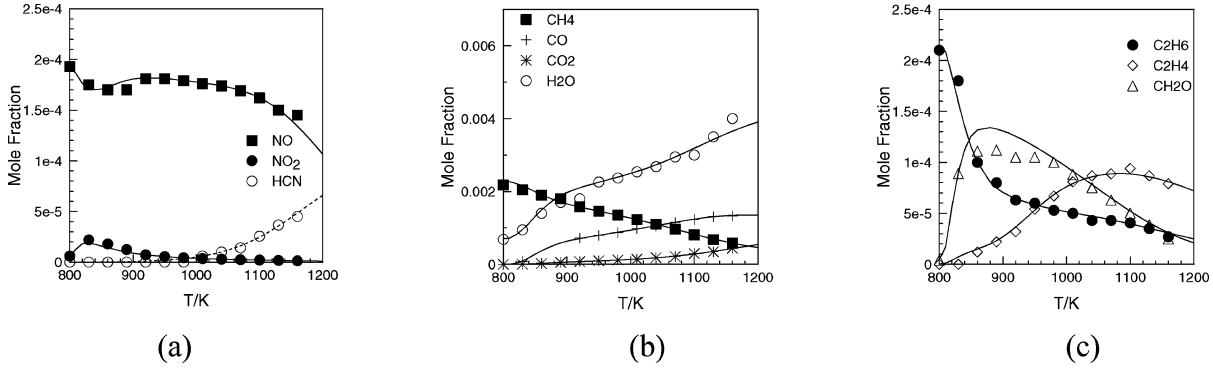

Figure 5. Mutual sensitization of the oxidation of a NGB (methane−ethane 10:1) and NO in a JSR at 10 atm: Effect of the introduction of 200 ppm of NO on the oxidation of methane in fuel-rich conditions ($\varphi = 1.5$, 2283 ppm of CH_4, 217 ppm of C_2H_6, 3550 ppm of O_2, $t = 800$ ms. The symbols and the continuous lines refer respectively to the data and the simulations (proposed scheme).

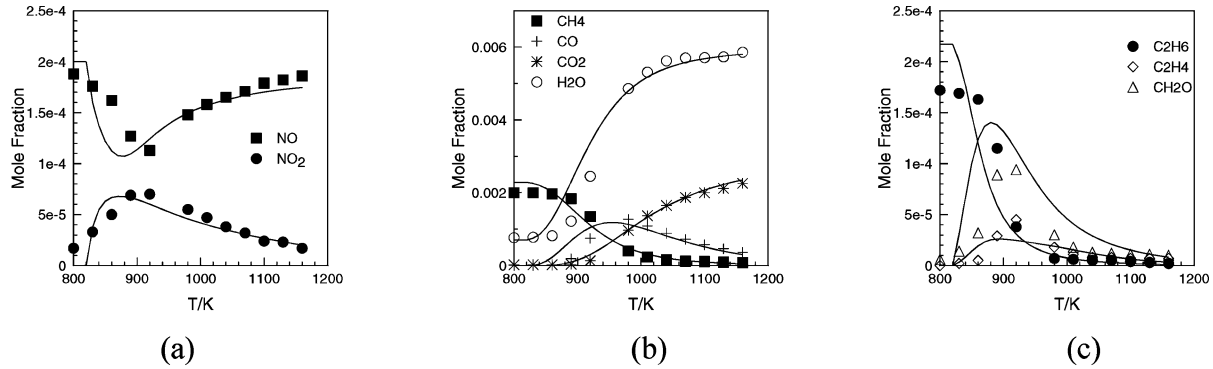

Figure 6. Mutual sensitization of the oxidation of a NGB (methane−ethane 10:1) and NO in a JSR at 10 atm: Effect of the introduction of 200 ppm of NO on the oxidation of methane under fuel-lean conditions ($\varphi = 0.3$, 2283 ppm of CH_4, 217 ppm of C_2H_6, 17751 ppm of O_2, $t = 250$ ms. The symbols and the continuous lines refer respectively to the data and the simulations (proposed scheme).

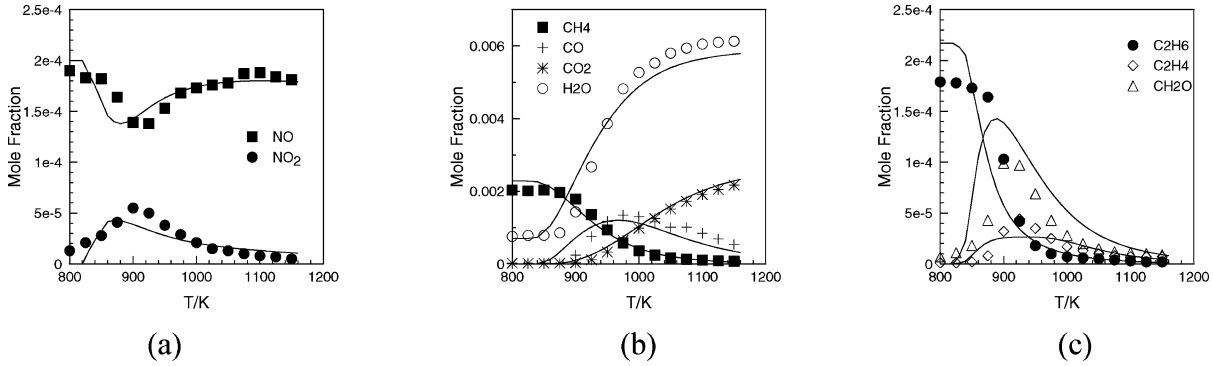

Figure 7. Mutual sensitization of the oxidation of a NGB (methane−ethane 10:1) and NO in a JSR at 10 atm: Effect of the introduction of 200 ppm of NO on the oxidation of methane under fuel-lean conditions ($\varphi = 0.5$, 2283 ppm of CH_4, 217 ppm of C_2H_6, 10700 ppm of O_2, $t = 250$ ms. The symbols and the continuous lines refer respectively to the data and the simulations (proposed scheme).

The ethylperoxy radicals almost entirely react with NO via reaction 1054, producing ethoxy radicals that decompose via two channels.

$$C_2H_5O_2 + NO \rightleftarrows C_2H_5O + NO_2; \quad R(C_2H_5O_2) = -1 \tag{1054}$$

$$C_2H_5O \rightleftarrows CH_3CHO + H; \quad R(C_2H_5O) = -0.62 \tag{1019}$$

$$C_2H_5O \rightleftarrows CH_3 + CH_2O; \quad R(C_2H_5O) = -0.38 \tag{1020}$$

Acetaldehyde, formed in reaction 1019 reacts via H atom abstraction by O_2, OH, and H yielding CH_3CO that in turn decomposes.

$$CH_3CO + M \rightleftarrows CH_3 + CO + M \tag{513}$$

At 900 K, where the NO_2 mole fraction is high, NO mostly reacts with HO_2 (88.7%), and to a lesser extent with CH_3O_2 (8.7%) and ethylperoxy (1.2%). HO_2 is still mostly produced (50%) by reaction 290 and also (46%) via reaction 314

$$HCO + O_2 \rightleftarrows HO_2 + CO \tag{314}$$

whereas it mostly reacts with NO (95.3%) via reaction 144. NO is recycled via three reactions:

$$NO_2 + H \rightleftarrows NO + OH \quad (32\%) \tag{149}$$

$$NO_2 + CH_3 \rightleftarrows NO + CH_3O \quad (52\%) \tag{1025}$$

$$NO_2 + C_2H_5 \rightleftarrows NO + C_2H_5O \quad (7\%) \tag{1051}$$

It is interesting to evaluate the relative importance of the routes

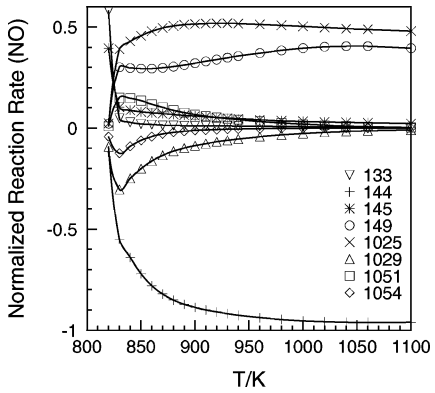

Figure 8. Normalized rates of reaction of NO at 10 atm (conditions of Figure 6). Reactions: $HNO + NO_2 \rightleftarrows NO + HONO$ (133); $NO + HO_2 \rightleftarrows NO_2 + OH$ (144); $NO + OH + M \rightleftarrows HONO + M$ (145); $NO_2 + H \rightleftarrows NO + OH$ (149); $CH_3 + NO_2 \rightleftarrows CH_3O + NO$ (1025); $CH_3O_2 + NO \rightleftarrows CH_3O + NO_2$ (1029); $C_2H_5 + NO_2 \rightleftarrows C_2H_5O + NO$ (1051); $C_2H_5O_2 + NO \rightleftarrows C_2H_5O + NO_2$ (1054).

to HO_2 from methane and ethane. That can be done via a reaction path analysis. Such computations show that the following sequence of reactions was responsible for the formation of H: $HCO + M \rightarrow H + CO + M$ (13%) and $CH_3O + M \rightarrow CH_2O + H + M$ (66%) were the most important reactions. The production of HCO and of CH_3 are strongly related. A simple scheme can be drawn from a "backwards reaction path analysis": ca. 12% of the methyl radicals come from ethane and ca. 86% from methane. The conversion of the methyl radical then follows the path $CH_3 \Rightarrow CH_3O \Rightarrow CH_2O \Rightarrow HCO$. CH_2O is also produced by oxidation of vinyl and vinyloxy radicals produced via the oxidation of ethane. It is therefore evident that the reactions of ethane significantly participate to the mutual sensitization of the oxidation of NO and a NGB here.

Methane is still consumed via reaction 322 and ethane through reaction 411. Methyl radicals react with NO_2 (81%) via (1025) and with oxygen (14.7%) via (988). Methoxy radicals mostly decompose via (390), yielding formaldehyde that reacts with OH (93%) via (404), yielding HCO that mostly reacts with oxygen (78%), producing HO_2. Hydroxyl radicals are responsible for methane oxidation; 95% of OH are produced via (144). The oxidation of ethane yields ethyl radicals that react with molecular oxygen producing ethene and HO_2 (14.5%), $C_2H_4O_2H$ (13%), and $C_2H_5O_2$ (12%). $C_2H_4O_2H$ decomposes to ethene and HO_2 whereas $C_2H_5O_2$ reacts with NO through reaction 1054.

At 1000 K, by which temperature, the formation of NO_2 has already declined, methane is still mainly consumed by OH (95.4%). At this temperature, methyl radicals mostly react with NO_2 (91%) via (1025), yielding CH_3O. Methoxy radicals mainly decompose (99%) in (390) yielding formaldehyde that reacts with OH (93%) to produce HCO. Formyl radicals are responsible for 33% of the formation of HO_2 via reaction 314 whereas this formation is dominated (64%) by reaction 290. At this temperature, NO mostly reacts with HO_2 (95%) via (144). Figure 8 gives the evolution of the importance of the major reactions consuming and recycling NO as a function of temperature (conditions of Figure 6). This figure clearly shows that increasing the temperature favors reaction 144 at the expense of reactions 1029 and 1054.

Sensitivity analyses were also performed (Figure 9) and showed that, at 900 K (conditions of Figure 6), the computed NO_2 concentrations are mainly sensitive to the kinetics of reactions 144, 149, 290, 1025, and 1029. At this temperature, reactions 144 and 1029 are the main routes to NO_2 formation. Reaction 290 produces HO_2 necessary to NO_2 formation via (144). Reactions 149 and 1025 have negative sensitivity coefficients since they remove 84% of NO_2.

It is also interesting to probe the effect of higher hydrocarbons on the kinetics of oxidation of methane and the combine effect of NO and higher hydrocarbons on the kinetics of methane oxidation. Therefore, we simulated the neat oxidation of methane, of the NGB mixture, and the oxidation of the same fuels in the presence of 200 ppm of NO, for equivalence ratio in the range 0.5−2. The modeling clearly showed the activating effect of ethane upon the oxidation of methane (Figure 10, parts a and c) and the sensitization of the oxidation of methane or the NGB by addition of NO (Figure 10, parts b and d). The most interesting result is that the addition of NO strongly reduces the difference of reactivity observed for methane and the NGB. Such an important result was not reported before and needed to be rationalized through a kinetic analysis.

Without NO, the oxidation of ethane starts at a lower temperature than that of methane, activating the oxidation of methane in the NGB mixture through easier production of radicals, as reported before.[22,23] In the conditions of Figure 9a, the oxidation of methane proceeds by reaction with OH radicals as indicated using rates of consumption/production analyses.

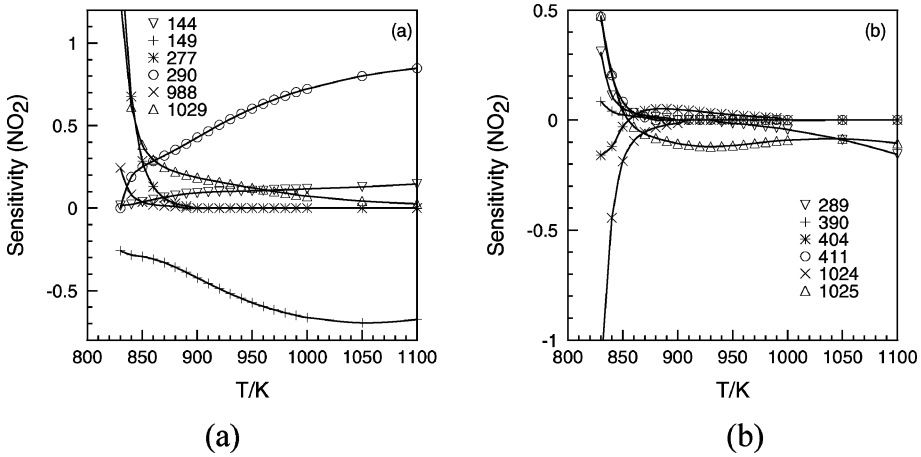

Figure 9. Sensitivity analysis results for NO_2 (conditions of Figure 6). Reactions: $NO + HO_2 \rightleftarrows NO_2 + OH$ (144); $NO_2 + H \rightleftarrows NO + OH$ (149); $CH_2O + NO_2 \rightleftarrows HCO + HONO$ (277); $H + O_2 \rightleftarrows OH + O$ (289); $H + O_2 + M \rightleftarrows HO_2 + M$ (290); $CH_3O + M \rightleftarrows CH_2O + H + M$ (390); $CH_2O + OH \rightleftarrows HCO + H_2O$ (404); $C_2H_6 + OH \rightleftarrows C_2H_5 + H_2O$ (411); $CH_3 + O_2(+M) \rightleftarrows CH_3O_2(+M)$ (988); $CH_3NO_2(+M) \rightleftarrows CH_3 + NO_2(+M)$ (1024); $CH_3 + NO_2 \rightleftarrows CH_3O + NO$ (1025); $CH_3O_2 + NO \rightleftarrows CH_3O + NO_2$ (1029).

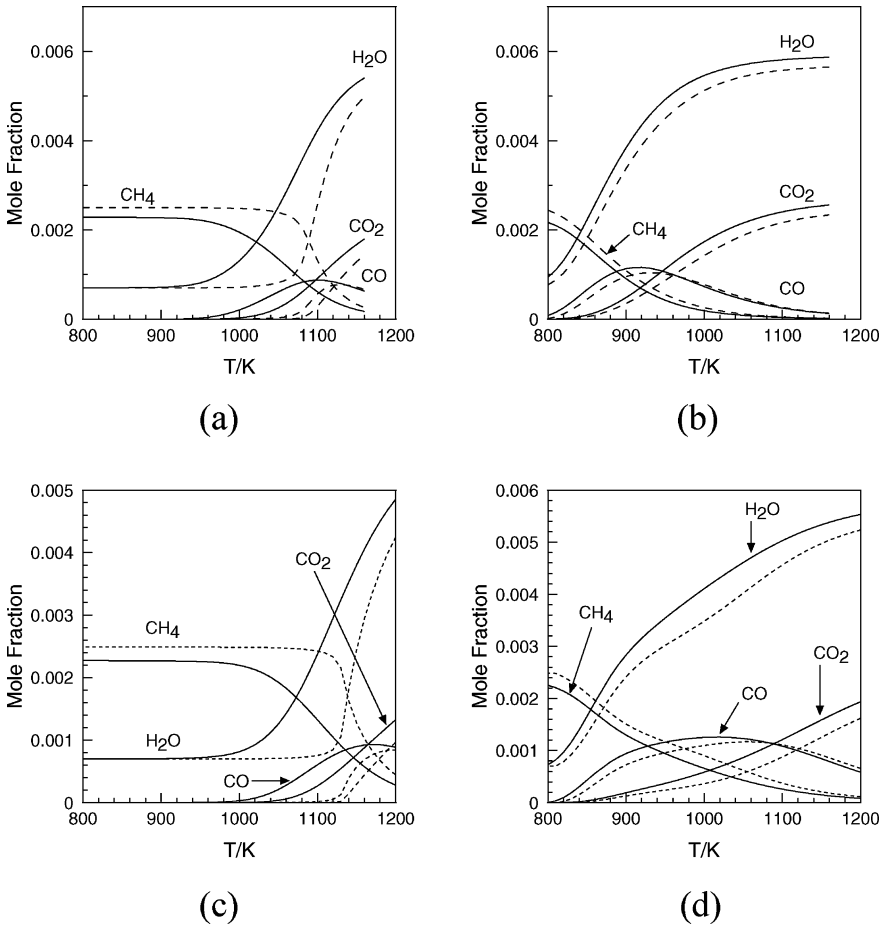

Figure 10. Comparison of the reactivity of methane and a NGB mixtures in a JSR at 10 atm and 0.8 s. (a) Full line: 2500 ppm of NGB ($\varphi = 0.5$, 2283 ppm of CH_4, 217 ppm of C_2H_6). Dashed line: 2500 ppm of CH_4. (b) Full line: 2500 ppm of NGB ($\varphi = 0.5$, 2283 ppm of CH_4, 217 ppm of C_2H_6), 200 ppm of NO. Dashed line: 2500 ppm of CH_4 and 200 ppm of NO. (c) Full line: 2500 ppm of NGB ($\varphi = 1$, 2283 ppm of CH_4, 217 ppm of C_2H_6). Dashed line: 2500 ppm of CH_4. (d) Full line: 2500 ppm of NGB ($\varphi = 1$, 2283 ppm of CH_4, 217 ppm of C_2H_6), 200 ppm of NO. Dashed line: 2500 ppm of CH_4 and 200 ppm of NO.

At 940 K, the reaction paths for the oxidation of methane and that of the NGB were compared. The ROP or ROC are given below. Italic font is used for the NGB case. About 90% of methane reacts with OH in both cases:

$$CH_4 + OH \rightleftarrows CH_3 + H_2O; \quad R(CH_4) = -0.911/\mathit{-0.891} \tag{322}$$

OH radicals are mainly produced by decomposition of hydrogen peroxide and reaction of methyl radicals with molecular oxygen:

$$H_2O_2\ (+M) \rightleftarrows 2\ OH\ (+M); \quad R(OH) = 0.152/\mathit{0.618}(-300)$$

$$CH_3 + O_2 \rightleftarrows CH_2O + OH; \quad R(OH) = 0.761/\mathit{0.142} \tag{338}$$

It is noticeable that the relative importance of the reactions yielding OH differs from one fuel mixture to the other. Hydrogen peroxide is produced by reaction of hydroperoxyl radicals:

$$2HO_2 \rightleftarrows H_2O_2 + O_2; \quad R(H_2O_2) = 0.226/\mathit{0.704} \tag{299}$$

$$CH_4 + HO_2 \rightleftarrows CH_3 + H_2O_2; \quad R(H_2O_2) = 0.624/\mathit{0.080} \tag{321}$$

$$CH_2O + HO_2 \rightleftarrows HCO + H_2O_2; \quad R(H_2O_2) = 0.149/\mathit{0.192} \tag{403}$$

The production of hydroperoxyl radicals mainly involved two reactions of comparable importance for the two fuels:

$$H + O_2 + M \rightleftarrows HO_2 + M; \quad R(HO_2) = 0.624/\mathit{0.549} \tag{290}$$

$$HCO + O_2 \rightleftarrows CO + HO_2; \quad R(HO_2) = 0.263/\mathit{0.159} \tag{314}$$

In the case of the NGB, an additional production of HO_2 occurs via

$$C_2H_5 + O_2 \rightleftarrows C_2H_4 + HO_2; \quad R(HO_2) = 0.0/\mathit{0.158} \tag{425}$$

$$C_2H_5 + O_2 \rightleftarrows C_2H_4O_2H \rightleftarrows C_2H_4 + HO_2;$$
$$R(HO_2) = 0.0/\mathit{0.120}(426,-432)$$

increasing the radical pool. These reactions are of negligeable importance when methane is the fuel, as demonstrated by the above-mentioned $R(HO_2) = 0$. The rate of consumption of methane is ca. 24 times higher for the NGB mixture than for neat methane, resulting from a higher rate of production of OH (ca. 37 times higher) in the NGB case.

In presence of NO (Figure 10, parts b and d), the reactions of NO with HO_2 radicals yield OH radicals readily, resulting in an improved oxidation of the fuel. As a result, there is less difference in the importance of the reaction paths for the

oxidation of methane and the NGB than in absence of NO, as shown by the kinetic modeling.

Under the conditions of Figure 10b, about 98% of methane reacts with OH in both cases:

$$CH_4 + OH \rightleftarrows CH_3 + H_2O; \quad R(CH_4) = -0.981/-0.978 \tag{322}$$

OH radicals are mainly produced by reaction of NO with HO_2:

$$NO + HO_2 \rightleftarrows NO_2 + OH\ (+M); \quad R(OH) = 0.670/0.637 \tag{144}$$

$$NO_2 + H \rightleftarrows NO + OH; \quad R(OH) = 0.222/0.265 \tag{149}$$

The relative importance of these reactions does not significantly depend on the composition of the fuel. The production of hydroperoxyl radicals mainly involves two reactions of comparable importance whether the fuel is methane or the NGB:

$$H + O_2 + M \rightleftarrows HO_2 + M; \quad R(HO_2) = 0.700/0.558 \tag{290}$$

$$HCO + O_2 \rightleftarrows CO + HO_2; \quad R(HO_2) = 0.273/0.377 \tag{314}$$

In the case of the NGB, an additional minor production of HO_2 occurs via

$$C_2H_5 + O_2 \rightleftarrows C_2H_4 + HO_2; \quad R(HO_2) = 0.0/0.017 \tag{425}$$

$$C_2H_5 + O_2 \rightleftarrows C_2H_4O_2H \rightleftarrows C_2H_4 + HO_2; \quad R(HO_2) = 0.0/0.023(426,-432)$$

increasing slightly the radical pool. The production of ethyl radicals from methane is much less important than from the NGB in the present conditions. Therefore, the ethylperoxy reactions are only significant during the NGB oxidation. The computed rate of consumption of methane is ca. 2 times higher for the NGB mixture than for neat methane, resulting from a higher rate of production of OH (ca. 3.6 times higher for the oxidation of the NGB). Therefore, there is much less difference of reactivity between methane and the NGB in the presence of NO than for the neat oxidation of the same fuel mixtures. Such a result is of importance since the composition of natural gas is not guaranteed by gas companies. These results show that operating with exhaust gas recirculation containing NO, such as in HCCI engines and flameless burners, can reduce the sensitivity of the combustion to the fuel composition.

5. Conclusion

New data were obtained for the mutual sensitization of the oxidation of NO and a NGB mixture (methane−ethane 10:1) in a JSR at10 atm, over the temperature range 800−1160 K, for fuel-lean to fuel-rich conditions. Sonic probe sampling with on-line FTIR analyses and off-line GC-TCD/FID analyses were used to measure the concentration profiles of the reactants, stable intermediates, and final products. A detailed chemical kinetic scheme, validated for the mutual sensitization of the oxidation of NO and methane, ethane, and ethene, was proposed for modeling these experiments. An overall good agreement between the data and the modeling was obtained. According to this model, the mutual sensitization of the oxidation of a NGB and NO proceeds through the NO to NO_2 conversion by HO_2, CH_3O_2, and to lesser extent by $C_2H_5O_2$. The $NO-NO_2$ conversion by CH_3O_2 + NO and $C_2H_5O_2$ + NO are more important at low temperatures (ca. 820 K) than at higher temperatures where the reaction of NO with HO_2 dominates. The NO to NO_2 conversion is enhanced by the production of HO_2 and alkylperoxy radicals from the oxidation of the fuel. The production of OH resulting from the oxidation of NO by HO_2 promotes the oxidation of the fuel. A simplified reaction scheme can be proposed: NO + HO_2 → OH followed by OH + CH_4 → CH_3 and OH + C_2H_6 → C_2H_5. At low-temperature, the reaction also proceeds via $CH_3 + O_2 \rightarrow CH_3O_2$; CH_3O_2 + NO → CH_3O + NO_2 and $C_2H_5 + O_2 \rightarrow C_2H_5O_2$; and $C_2H_5O_2$ + NO → C_2H_5O + NO_2. At higher temperature, methoxy radicals are produced via $CH_3 + NO_2 \rightarrow CH_3O$. The further reactions $C_2H_5O \rightarrow CH_3CHO + H$; $CH_3O \rightarrow CH_2O + H$; CH_2O + OH → HCO; HCO + O_2 → HO_2; and H + O_2 → HO_2 complete the sequence. This study shows that the higher hydrocarbons present in natural gas affect the kinetics of the mutual sensitization of the oxidation of NO and a NGB. The importance of the reactions of the ethylperoxy radical is not negligible although the concentration of ethane in the NGB represents only 10% of the fuel. It was also shown that the presence of NO reduces significantly the difference of reactivity between methane and a NGB mixture since the production of the main oxidation agent, OH, proceeds via the same route, NO + HO_2 → NO_2 + OH in both cases. These results further demonstrate the efficiency of traces of NO to activate the oxidation of relatively unreactive systems, or to avoid oxidation inhibition.[30]

Acknowledgment. This research was funded in part through the "Action Concertée Energie" of CNRS-MRNT-DGA, Contract "SYNGAZ-GTL-HCCI" and the Predit research program. G.D. thanks the SPI department of CNRS for a postdoctoral grant. The authors are grateful to I. Tilouh for his help with the experiments.

References and Notes

(1) Thompson, H. W.; Hinshelwood, C. N. *Proc. R. Soc.* **1928**, *A 124*, 219.

(2) Slack, M.; Grillo, A. *Investigation of hydrogen-air ignition sensitized by nitric oxide and by nitrogen dioxide*; NASA Report: NASA: Washington, DC, 1977; No. 2896.

(3) Bromly, J. H.; Barnes, F. J.; Nelson, P. F.; Haynes, B. S. *Int. J. Chem. Kinet.* **1995**, *27*, 1165−1178.

(4) Bromly, J. H.; Barnes, J. F.; Muris, S.; You, X.; Haynes, B. S. *Combust. Sci. Technol.* **1996**, *115*, 259−296.

(5) Bendtsen, A. B.; Glarborg, P.; Dam-Johansen, K. *Combust. Sci. Technol.* **2000**, *151*, 31−71.

(6) Doughty, A.; Barnes, F. J.; Bromly, J. H.; Haynes, B. S. *Proc. Combust. Inst.* **1996**, *26*, 589−596.

(7) Dagaut, P.; Lecomte, F.; Chevailler, S.; Cathonnet, M. *Combust. Sci. Technol.* **1999**, *148*, 27−57.

(8) Alzueta, M. U.; Muro, J.; Bilbao, R.; Glarborg, P. *Isr. J. Chem.* **1999**, *39*, 73−86.

(9) Dagaut, P.; Luche, J.; Cathonnet, M. *Combust. Sci. Technol.* **2001**, *165*, 61−84.

(10) Nelson, P. F.; Haynes, B. S. *Proc. Combust. Inst.* **1994**, *25*, 1003−1010.

(11) Hori, M.; Matsunaga, N.; Marinov, N. M.; Pitz, J. W.; Westbrook, C. K. *Proc. Combust. Inst.* **1998**, *27*, 389−396.

(12) Bromly, J. H.; Barnes, F. J.; Mandyczewsky, R.; Edwards, T. J.; Haynes, B. S. *Proc. Combust. Inst.* **1992,** *24*, 899−907.

(13) Hori, M.; Koshiishi, Y.; Matsunaga, N.; Glaude, P.; Marinov, N. *Proc. Combust. Inst.* **2002**, *29*, 2219−2226.

(14) Hori, M. *Proc. Combust. Inst.* **1986**, *21*, 1181−1188.

(15) Hori, M. *Proc. Combust. Inst.* **1988**, *22*, 1175−1181.

(16) Hori, M.; Matsunaga, N.; Malte, P. C.; Marinov, N. M. *Proc. Combust. Inst.* **1992**, *24*, 909−916.

(17) Konnov, A. A.; Barnes, F. J.; Bromly, J. H.; Zhu, J. N.; Zhang, D.-K. *Combust. Flame* **2005**, *141*, 191−199.

(18) Dagaut, P.; Nicolle, A. *Combust. Flame* **2005**, *140*, 161−171.

(19) Cavaliere, A.; de Joannon, M. *Prog. Energ. Combust. Sci.* **2004**, *30*, 329−366.

(20) Colin, O.; Pires da Cruz, A.; Jay, S. *Proc. Combust. Inst.* **2005**, *30*, 2649−2656.

(21) Moreac, G.; Dagaut, P.; Roesler, J.; Cathonnet, M. *Proc. Mediterranean Combust. Symp.* **2002**, *2*, 240−251.

(22) Tan, Y.; Dagaut, P.; Cathonnet, M.; Boettner, J.-C.; Bachman, J. S.; Carlier, P. *Proc. Combust. Inst.* **1994**, *25*, 1563−1569.

(23) Tan, Y.; Dagaut, P.; Cathonnet, M.; Boettner, J.-C. *Combust. Sci. Technol.* **1994**, *103*, 133−151.

(24) Smith, G. P.; Golden, D. M.; Frenklach, M.; Moriarty, N. W.; Eiteneer, B.; Goldenberg, M.; Bowman, C. T.; Hanson, R. K.; Song, S.; Gardiner, W. C., Jr.; Lissianski, V. V.; Qin, Z. http//www.berkeley.edu/gri-mech/1999.

(25) Dagaut, P.; Mathieu, O.; Nicolle, A.; Dayma, G. *Combust. Sci. Technol.* **2005**, *177*, 1767−1791.

(26) Dagaut, P.; Cathonnet, M.; Rouan, J.-P.; Foulatier, R.; Quilgars, A.; Boettner, J.-C.; Gaillard, F.; James, H. *J. Phys. E: Instrum.* **1985**, *19*, 207−209.

(27) Glarborg, P.; Kee, R. J.; Grcar, J. F.; Miller, J. A. *PSR: A FORTRAN program for modeling well-stirred reactors*; Report No. SAND86−8209; Sandia National Laboratories: Sandia, NM, 1986.

(28) Dagaut, P.; Lecomte, F.; Mieritz, J.; Glarborg, P. *Int. J. Chem. Kinet.* **2003**, *35*, 543−575.

(29) Curran, H. J.; Pitz, W. J.; Westbrook, C. K.; Dagaut, P.; Boettner, J.-C.; Cathonnet, M. *Int. J. Chem. Kinet.* **1998**, *30*, 229−241.

(30) Dagaut, P.; Nicolle, A. *Int. J. Chem. Kinet.* **2005**, *37*, 406−413.